
Article:
Giarè, W., Sabogal, M.A., Nunes, R.C. et al. (2024) Interacting dark energy after DESI baryon acoustic oscillation measurements. Physical Review Letters, 133 (25). 251003. ISSN: 0031-9007

https://doi.org/10.1103/physrevlett.133.251003

Interacting Dark Energy after DESI Baryon Acoustic Oscillation Measurements

William Giarè,[1,*] Miguel A. Sabogal,[2,†] Rafael C. Nunes,[2,3,‡] and Eleonora Di Valentino[1,§]
[1]School of Mathematics and Statistics, University of Sheffield, Hounsfield Road, Sheffield S3 7RH, United Kingdom
[2]Instituto de Física, Universidade Federal do Rio Grande do Sul, 91501-970 Porto Alegre RS, Brazil
[3]Divisão de Astrofísica, Instituto Nacional de Pesquisas Espaciais, Avenida dos Astronautas 1758, São José dos Campos, 12227-010, São Paulo, Brazil

(Received 29 April 2024; revised 14 June 2024; accepted 19 November 2024; published 18 December 2024)

We investigate the implications of the baryon acoustic oscillations measurement released by the Dark Energy Spectroscopic Instrument for interacting dark energy (IDE) models characterized by an energy-momentum flow from dark matter to dark energy. By combining Planck-2018 and Dark Energy Spectroscopic Instrument data, we observe a preference for interactions, leading to a nonvanishing interaction rate $\xi = -0.32^{+0.18}_{-0.14}$, which results in a present-day expansion rate $H_0 = 70.8^{+1.4}_{-1.7}$ km/s/Mpc, reducing the tension with the value provided by the SH0ES Collaboration to less than $\sim 1.3\sigma$. The preference for interactions remains robust when including measurements of the expansion rate $H(z)$ obtained from the relative ages of massive, early-time, and passively evolving galaxies, as well as when considering distance moduli measurements from Type Ia supernovae sourced from the Pantheon-plus catalog using the SH0ES Cepheid host distances as calibrators. Overall, the IDE framework provides an equally good, or better, explanation of both high- and low-redshift *background* observations compared to the lambda cold dark matter model, while also yielding higher H_0 values that align more closely with the local distance ladder estimates. However, a limitation of the IDE model is that it predicts lower Ω_m and higher σ_8 values, which may not be fully consistent with large-scale structure data at the *perturbation* level.

DOI: 10.1103/PhysRevLett.133.251003

The well-known discrepancy between the present-day expansion rate of the Universe (H_0) as measured by the SH0ES Collaboration using local distance ladder measurements from Type Ia supernovae [1–3] ($H_0 = 73 \pm 1$ km/s/Mpc), and the value of the same parameter inferred by the Planck Collaboration [4] from observations of temperature and polarization anisotropies in the cosmic microwave background (CMB) radiation, assuming a lambda cold dark matter (ΛCDM) cosmology ($H_0 = 67.4 \pm 0.5$ km/s/Mpc), has reached a statistical significance exceeding 5σ. Barring any possible systematic origin of this discrepancy [5], a fascinating possibility is that the Hubble tension might be pointing towards new physics beyond the standard ΛCDM model of cosmology.

Numerous theoretical attempts have been proposed to increase the value of H_0 inferred from CMB data and restore cosmic concordance [8–11]. However, a compelling solution to the problem remains elusive. The primary challenge stems from the highly precisely determined angular scale of the acoustic peaks in the CMB spectra [4]. This scale sets the ratio between the sound horizon at recombination and the angular diameter distance to the last scattering surface. Increasing the value of H_0 without disrupting the acoustic scale requires either a reduction in the value of the sound horizon or a different postrecombination expansion history of the Universe able to compensate for a higher H_0 while preserving the angular diameter distance from the last scattering surface [12].

Both of these possibilities face severe constraints. Reducing the value of the sound horizon requires new physics acting at very high redshifts, typically just prior to recombination. Even ignoring the common fine-tuned problems surrounding early-time solutions, they remain severely constrained by high redshift observations, most notably by CMB data [13]. Conversely, late-time solutions require new physics altering cosmic distances to compensate for the higher values of H_0 while preserving the angular diameter distance from the CMB. In turn, cosmic distances are precisely measured by baryon acoustic oscillations (BAO) and Type Ia supernovae (SN) data that so far have not provided any evidence for deviations from a late-time ΛCDM cosmology, significantly reducing the room allowed for new physics at low redshift [14–17].

*Contact author: w.giare@sheffield.ac.uk
†Contact author: miguel.sabogal@ufrgs.br
‡Contact author: rafadcnunes@gmail.com
§Contact author: e.divalentino@sheffield.ac.uk

Interestingly, recent BAO measurements released by the Dark Energy Spectroscopic Instrument [18–20] (DESI) appear to point toward new physics in the dark energy sector of the cosmological model [20]. Following the intrinsic interest sparked by these new observations [21–24], in this Letter, we examine their implications for cosmological models known as interacting dark energy (IDE) models, where a nongravitational interaction between dark matter (DM) and dark energy (DE) is postulated. Over the years, these models have been extensively explored as a potential avenue for resolving cosmological tensions [25–33]. Despite high-redshift data supporting IDE models as solutions to the Hubble tension [30], the situation remains somewhat unclear when examining low-redshift observations, as different probes yield somewhat discordant conclusions [33–35]. In this Letter, we demonstrate that the new DESI data give a preference for interactions exceeding the 95% confidence level (CL) and that high- and low-redshift *background* observations can be equally or better explained in IDE models than in ΛCDM, while yielding higher values of H_0 compatible with SH0ES.

We consider a homogeneous and isotropic Universe and introduce an energy-momentum flow in the dark sector of the model by modifying the energy-momentum equation as

$$\nabla_\mu T_i^{\mu\nu} = Q_i^\nu, \qquad \sum_i Q_i^\mu = 0. \tag{1}$$

The degree of interaction is quantified by the four-vector

$$Q_i^\mu = (Q_i + \delta Q_i)u^\mu + a^{-1}(0, \partial^\mu f_i), \tag{2}$$

where u^μ represents the velocity four-vector, Q_i is the background energy transfer, and the index i runs over DM and DE. We adopt a widely recognized interaction kernel $Q = \mathcal{H}\xi\rho_{\rm DE}$ [30,36–39] where $\mathcal{H}$ is the (conformal) Hubble parameter, $\rho_{\rm DE}$ is the DE energy density, and ξ dictates both the amount and the direction of energy-momentum flow. We require $\xi < 0$, forcing the energy-momentum transfer from DM to DE. Additionally, we fix the DE equation of state to $w \simeq -1$, resembling an interacting vacuum scenario [40].

We implement the theoretical model in a modified version of the Boltzmann solver code CLASS [42] and use the publicly available sampler COBAYA [43] to perform Markov chain Monte Carlo analyses. We assume flat priors on the set of sampled cosmological parameters $\{\Omega_b h^2$, $\Omega_c h^2$, $\tau_{\rm reio}$, $\theta_{\rm s}$, $\log(10^{10}A_{\rm s})$, $n_{\rm s}$, $\xi\}$. Our baseline datasets include the Planck-2018 CMB temperature polarization and lensing likelihoods [4,44,45] and the DESI BAO measurements obtained from observations of galaxies and quasars [18], and Lyman-α [19] tracers summarized in Table I of Ref. [20]. These latter are characterized in terms of measurements of the transverse comoving distance ($D_{\rm M}/r_{\rm d}$), the Hubble horizon ($D_{\rm H}/r_{\rm d}$), and the angle-averaged distance ($D_{\rm V}/r_{\rm d}$), normalized to the (comoving) sound horizon at the drag epoch, $r_{\rm d}$. We account for the correlation between measurements of $D_{\rm M}/r_{\rm d}$ and $D_{\rm H}/r_{\rm d}$. In addition to CMB and BAO data, we also consider distance moduli measurements from Type Ia SN gathered from the Pantheon-plus sample [46]. For this Letter we use the SH0ES Cepheid host distances as calibrators [1]. Finally, we include measurements of the expansion rate $H(z)$ derived from the relative ages of massive, early-time, passively evolving galaxies, known as cosmic chronometers (CC) [47]. We conservatively use only 15 CC measurements in the redshift range $0.179 < z < 1.965$ [48–50], accounting for all nondiagonal terms in the covariance matrix and systematic contributions.

We summarize the constraints on cosmological parameters at 68% and 95% CL in Table I. The most important results read as follows. First, the joint Planck + DESI analysis yields a preference for a nonvanishing $\boldsymbol{\xi = -0.32^{+0.18}_{-0.14}}$, exceeding the 95% CL. Additionally, it provides a value $H_0 = 70.8^{+1.4}_{-1.7}$ km/s/Mpc, in agreement with local distance ladder estimates within $\sim 1.3\sigma$. Therefore, focusing on Planck-2018 and DESI-BAO altogether, the IDE model can fully resolve the Hubble tension; see also Fig. 1. Adding CC does not change this result; see also Table I. That said, as shown in Table I, the IDE model predicts lower Ω_m and higher σ_8 values, which suggest potential challenges in providing a consistent description of large-scale structure data at the perturbation level. We discuss this aspect in more detail at the end of this Letter, where we analyze the impact of redshift space distortion (RSD) measurements and highlight some limitations of the IDE framework.

Second, combining Planck-2018 + DESI + SN, we still find a preference for $\xi \neq 0$ at more than 95% CL, consistently yielding values of H_0 higher than in the standard cosmological model; see also Table I and Fig. 1. Again, this conclusion does not change considering CC. A nonvanishing energy-momentum flow from DM to DE is potentially supported by *all* the main high- and low-redshift background measurements analyzed in this work.

Third, for all the datasets listed in Table I, we compare the best-fit $\chi^2_{\rm IDE}$ obtained within the IDE model to the best-fit $\chi^2_{\Lambda\rm CDM}$ obtained for the ΛCDM model. We find that $\Delta\chi^2 = \chi^2_{\rm IDE} - \chi^2_{\Lambda\rm CDM}$ is always negative. This means that the IDE model can fit data better than the ΛCDM model for *all* the different combinations of data while simultaneously yielding higher values of H_0.

Fourth, to account for the fact that the IDE model has one more free parameter than the ΛCDM model, we perform a model comparison and calculate the Bayes factors $\ln \mathcal{B}_{ij}$ normalized (for each dataset) to a baseline ΛCDM scenario in such a way that a negative $\ln \mathcal{B}_{ij}$ indicates a preference for the IDE model over the ΛCDM model and vice versa [51]. Despite a trend toward $\ln \mathcal{B}_{ij} < 0$, the evidence is always inconclusive. Therefore, we conclude that IDE and

TABLE I. Constraints at 68% (95%) CL on the parameters of the IDE model. For all datasets, we provide $\Delta\chi^2 = \chi^2_{\rm IDE} - \chi^2_{\Lambda\rm CDM}$ as well as the Bayes factors $\ln\mathcal{B}_{ij} = \ln\mathcal{Z}_{\Lambda\rm CDM} - \ln\mathcal{Z}_{\rm IDE}$ calculated as the difference between the evidence for the ΛCDM and IDE models. Negative values of $\Delta\chi^2$ and $\ln\mathcal{B}_{ij}$ indicate a better fit and a preference for the IDE model over the ΛCDM, respectively.

Parameter	Planck-2018 + DESI	Planck-2018 + DESI + CC	Planck-2018 + DESI + SN	Planck-2018 + DESI + SN + CC
$\Omega_b h^2$	$0.022\,43 \pm 0.000\,14 (0.022\,43^{+0.000\,28}_{-0.000\,26})$	$0.022\,43 \pm 0.000\,14 (0.022\,43^{+0.000\,27}_{-0.000\,27})$	$0.022\,54 \pm 0.000\,13 (0.022\,54^{+0.000\,26}_{-0.000\,27})$	$0.022\,55 \pm 0.000\,14 (0.022\,55^{+0.000\,27}_{-0.000\,27})$
$\Omega_c h^2$	$0.079^{+0.025}_{-0.016} (0.079^{+0.037}_{-0.042})$	$0.080^{+0.025}_{-0.016} (0.080^{+0.037}_{-0.042})$	$0.0962^{+0.0085}_{-0.0074} (0.096^{+0.015}_{-0.015})$	$0.0966^{+0.0084}_{-0.0075} (0.097^{+0.015}_{-0.016})$
$100\theta_s$	$1.041\,98 \pm 0.000\,29 (1.041\,98^{+0.000\,56}_{-0.000\,56})$	$1.041\,97 \pm 0.000\,28 (1.041\,97^{+0.000\,54}_{-0.000\,56})$	$1.042\,11 \pm 0.000\,28 (1.042\,11^{+0.000\,55}_{-0.000\,57})$	$1.042\,11 \pm 0.000\,28 (1.042\,11^{+0.000\,54}_{-0.000\,54})$
$\tau_{\rm reio}$	$0.0555 \pm 0.0074 (0.055^{+0.015}_{-0.014})$	$0.0554^{+0.0069}_{-0.0078} (0.055^{+0.016}_{-0.014})$	$0.0592^{+0.0069}_{-0.0079} (0.059^{+0.016}_{-0.014})$	$0.0590 \pm 0.0077 (0.059^{+0.016}_{-0.015})$
n_s	$0.9672 \pm 0.0037 (0.9672^{+0.0073}_{-0.0072})$	$0.9673 \pm 0.0037 (0.9673^{+0.0074}_{-0.0073})$	$0.9696 \pm 0.0038 (0.9696^{+0.0075}_{-0.0073})$	$0.9693 \pm 0.0038 (0.9693^{+0.0073}_{-0.0076})$
$\log(10^{10}A_s)$	$3.045 \pm 0.014 (3.045^{+0.029}_{-0.028})$	$3.045^{+0.014}_{-0.015} (3.045^{+0.030}_{-0.028})$	$3.051 \pm 0.015 (3.051^{+0.031}_{-0.028})$	$3.050^{+0.014}_{-0.016} (3.050^{+0.031}_{-0.029})$
ξ	$-0.32^{+0.18}_{-0.14} (-0.32^{+0.30}_{-0.29})$	$-0.32^{+0.18}_{-0.14} (-0.32^{+0.30}_{-0.28})$	$-0.186 \pm 0.068 (-0.19^{+0.13}_{-0.14})$	$-0.183 \pm 0.069 (-0.18^{+0.13}_{-0.14})$
H_0 [km/s/Mpc]	$70.8^{+1.4}_{-1.7} (70.8^{+2.8}_{-2.7})$	$70.7^{+1.4}_{-1.7} (70.7^{+2.9}_{-2.7})$	$69.87 \pm 0.60 (69.9^{+1.2}_{-1.2})$	$69.83 \pm 0.59 (69.8^{+1.2}_{-1.1})$
Ω_m	$0.206^{+0.056}_{-0.044} (0.206^{+0.090}_{-0.096})$	$0.208^{+0.057}_{-0.043} (0.208^{+0.090}_{-0.097})$	$0.245 \pm 0.020 (0.245^{+0.037}_{-0.039})$	$0.246 \pm 0.020 (0.246^{+0.038}_{-0.040})$
σ_8	$1.23^{+0.14}_{-0.36} (1.23^{+0.74}_{-0.52})$	$1.220^{+0.082}_{-0.36} (1.22^{+0.70}_{-0.45})$	$0.974^{+0.059}_{-0.088} (0.97^{+0.15}_{-0.14})$	$0.971^{+0.060}_{-0.086} (0.97^{+0.15}_{-0.14})$
$r_{\rm drag}$ [Mpc]	$147.28 \pm 0.23 (147.28^{+0.45}_{-0.45})$	$147.28 \pm 0.24 (147.28^{+0.46}_{-0.46})$	$147.42 \pm 0.23 (147.42^{+0.44}_{-0.46})$	$147.40 \pm 0.23 (147.40^{+0.44}_{-0.45})$
$\Delta\chi^2$	−1.02	−2.00	−2.27	−2.21
$\ln\mathcal{B}_{ij}$	−0.10	−0.47	−0.32	−0.01

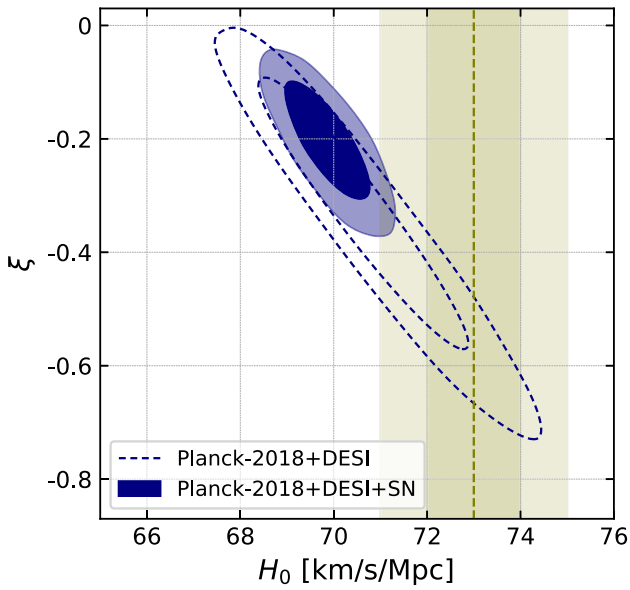

FIG. 1. 2D contours at 68% and 95% CL for the coupling parameter ξ and the Hubble parameter H_0, as inferred by the different combinations of Planck-2018, DESI, and SN data listed in the legend. The olive-green band represents the value of H_0 measured by the SH0ES Collaboration.

ΛCDM models can be deemed equally plausible to fit current observations.

Taking the results obtained by combining Planck-2018 and DESI BAO distance measurements at face value, there is solid ground to conclude that they lend weight to the possibility of nonvanishing energy-momentum transfer from DM to DE, resulting in the pronounced negative correlation between ξ and H_0 depicted in Fig. 1. This preference can be better understood by referring to Ref. [20]. In this work, the DESI Collaboration argued that considering a dynamical w_0w_aCDM parametrization, Planck-2018 + DESI data produce a strong preference for a (dynamical) DE equation of state showing a phantom behavior in the past. In the IDE model, upon straightforward manipulation of the continuity equation, one can rearrange the effective equation of state parameters to be $w_{\rm eff} = -1 + \xi/3$. Consequently, the preference for a late-time phantomlike behavior is recast into an indication $\xi < 0$ here exceeding the 95% CL. Focusing on Planck + DESI(+CC), this preference can fully resolve the Hubble tension. However, the significant fraction of energy-momentum transferred from DM to DE naturally implies lower values of the matter density parameter (Ω_m), and predicts a larger value of the variance in the mass distribution smoothed over a spherical volume of radius $R = 8\ h^{-1}$Mpc (σ_8) compared to the standard cosmological model. When SN data are included in the analysis, we observe a tendency toward higher values of Ω_m that reduces the value inferred for H_0. Having said that, despite a larger Ω_m, H_0 remains in better agreement with SH0ES, reducing

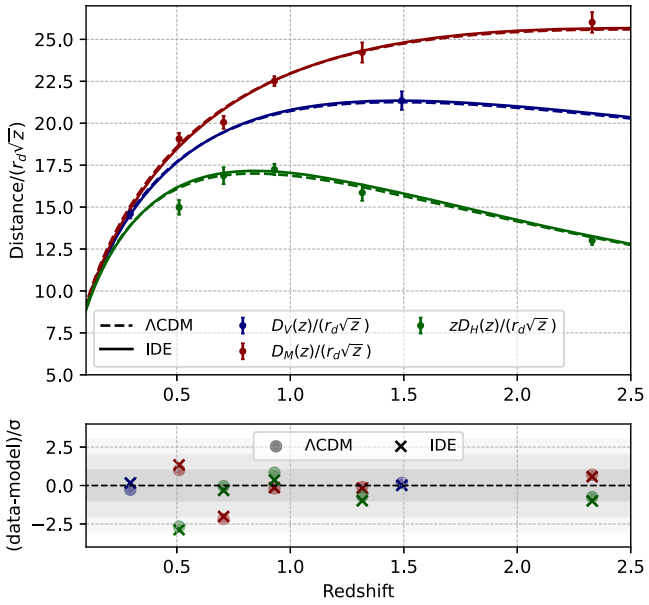

FIG. 2. Upper panel: best-fit predictions for (rescaled) distance-redshift relations for IDE (solid curves) and ΛCDM (dashed curves) models obtained from the analysis of Planck-2018 + DESI data. These predictions are presented for the three different types of distances probed by BAO measurements, each indicated by the colors reported in the legend. The error bars represent $\pm 1\sigma$ uncertainties. Lower panel: difference between the model prediction and data point for each BAO measurement, normalized by the observational uncertainties. The IDE model predictions are represented by x's, while the ΛCDM model predictions are represented by bullets.

TABLE II. The DESI results (and their 1σ errors) are presented for three distinct types of distances investigated by BAO measurements. For each data point, we indicate the consistency between the best-fit predictions of the IDE and ΛCDM models and the observed data, expressed in units of observational uncertainties ($\#\sigma$).

Distance	Redshift	DESI	IDE ($\#\sigma$)	ΛCDM ($\#\sigma$)
$D_V(z)/(r_d\sqrt{z})$	0.295	14.60 ± 0.28	$+0.16\sigma$	-0.28σ
	1.491	21.35 ± 0.55	$+0.01\sigma$	$+0.17\sigma$
$D_M(z)/(r_d\sqrt{z})$	0.510	19.07 ± 0.35	$+1.34\sigma$	$+1.01\sigma$
	0.706	20.05 ± 0.38	-2.02σ	-2.18σ
	0.930	22.51 ± 0.29	-0.14σ	-0.19σ
	1.317	24.22 ± 0.60	-0.17σ	-0.11σ
	2.330	26.01 ± 0.61	$+0.57\sigma$	$+0.70\sigma$
$zD_H(z)/(r_d\sqrt{z})$	0.510	14.98 ± 0.43	-2.87σ	-2.67σ
	0.706	16.87 ± 0.50	-0.32σ	-0.03σ
	0.930	17.24 ± 0.34	$+0.35\sigma$	$+0.84\sigma$
	1.317	15.86 ± 0.48	-0.99σ	-0.69σ
	2.330	13.00 ± 0.25	-1.00σ	-0.75σ

the Hubble tension to 2.6σ. Therefore, while within the ΛCDM model, forcing H_0 to move toward the SH0ES value leaves little room for agreement with local distance ladder estimates, the IDE model could offer a more flexible theoretical framework [54].

To better understand the role played by DESI data, we compare the theoretical distance predictions for IDE and ΛCDM models against the observed cosmic distances. In particular, in Fig. 2, we compare the Planck-2018 + DESI best-fit predictions for the three different types of (rescaled) distances probed by BAO measurements. In the bottom panel of the same figure, we show the distance between the observed DESI data points and the best-fit predictions obtained for the ΛCDM model (bullets) and the IDE model (x's) in units of observational uncertainty σ. The same difference between the model predictions and DESI data is summarized in Table II. Comparing the best-fit predictions for IDE and ΛCDM, some important conclusions can be reached. Foremost, we observe that the DESI data point showing the largest disagreement with the IDE model (at a level of approximately 2.9σ) is the measurement of $zD_H(z)/(r_d\sqrt{z})$ at $z = 0.510$. The only other DESI BAO measurement displaying a significant deviation from the IDE best-fit curve (at approximately 2σ) is $D_M(z)/(r_d\sqrt{z})$ at $z = 0.706$. However, these two data points also exhibit significant disagreement with the ΛCDM model (at approximately 2.7σ and 2.2σ, respectively). Therefore, the IDE model explains $D_M(z)/(r_d\sqrt{z})$ at $z = 0.706$ more successfully than the ΛCDM model. Overall, apart from these two distance measurements at $z = 0.51$ and $z = 0.706$ (which, *repetita iuvant*, are also at odds with the ΛCDM model), there are no other BAO measurements in tension with the IDE best-fit predictions. Last but not least, we stress that a large part of the improvement in the total $\Delta\chi^2 = -1.02$ over the ΛCDM model, as shown in Table I for Planck-2018 + DESI, comes specifically from the DESI BAO measurement ($\Delta\chi^2_{\rm DESI} = -0.73$).

In Fig. 3, we present the theoretical predictions for $H(z)$ as obtained by simultaneously analyzing Planck-2018, DESI, CC, and SN. We display the best-fit predictions (along with their 1 and 2σ uncertainties) for the IDE and ΛCDM models, comparing them against the data points released by DESI. As evident from the figure, even accounting for all datasets together, the DESI data point at $z = 0.51$ remains essentially unexplained in both models. Conversely, the IDE model can fit $H(z)$ at $z = 0.706$ and $z = 0.930$ better than the ΛCDM model, simultaneously predicting a larger present-day expansion rate H_0, as evident when comparing the red and blue reconstructed curves at $z = 0$. [In the Appendix, we briefly discuss a comparative study using the DESI and SDSS collaboration samples (complete BOSS + eBOSS sample)].

In this Letter, we have studied the implications of the baryon acoustic oscillation measurements released by the Dark Energy Spectroscopic Instrument for interacting

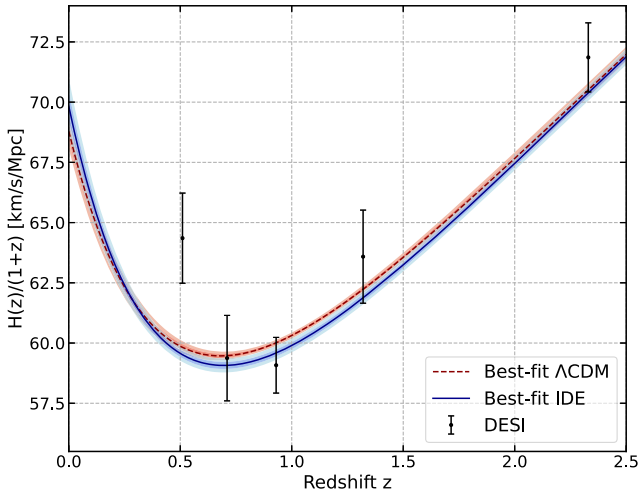

FIG. 3. Statistical reconstruction of the (rescaled) expansion rate of the Universe $H(z)/(1+z)$ at 1σ and 2σ confidence levels for the ΛCDM and IDE models through the joint analysis of Planck-2018 + DESI + SN + CC, compared to DESI measurements.

dark energy models characterized by an energy-momentum flow from dark matter to dark energy. Focusing on the minimal Planck-2018 + DESI data combination, we found a preference for interactions exceeding the 95% confidence level, yielding a present-day expansion rate $H_0 = 70.8^{+1.4}_{-1.7}$ km/s/Mpc that can resolve the Hubble tension. Combining Planck-2018 + DESI with either measurements of the expansion rate $H(z)$ obtained from the relative ages of massive, early-time, and passively evolving galaxies or with distance moduli measurements from Type Ia Supernovae sourced from the Pantheon-plus catalog using the SH0ES Cepheid host distances as a calibrator, we still find a preference for $\xi \neq 0$ at more than 95% CL. For all the different combinations of datasets, we observe an improvement in the χ^2 of the fit over the ΛCDM model. Overall, accounting for DESI data, high and low redshift background measurements are found to be equally or better explained within the IDE framework than the ΛCDM, while consistently yielding values of H_0 that are higher than in the standard cosmological model and in much better agreement with local distance ladder estimates.

In light of these results, we conclude that DESI data (re)open the possibility of addressing the Hubble tension through late-time new physics. However, we emphasize that our analysis of large-scale structure data primarily focused on distance measurements from DESI BAO and Type Ia SN. An important next step is to check whether the model satisfies constraints related to structure formation. In this context, the growth rate of matter density perturbations derived from peculiar velocities, associated with RSD, is commonly used to constrain the combination $f(z)\sigma_8(z)$, which can significantly influence the class of models considered here. Although RSD measurements from the DESI Collaboration have not yet been released, we extend our analysis to include 22 measurements of $f\sigma_8(z)$ spanning the redshift range $0.02 < z < 1.944$, gathered from various surveys and summarized in Table I of Ref. [55]. The analysis of RSD measurements provides substantial additional information for constraining the IDE framework, thereby strengthening the constraints and limiting the interaction parameter. Using RSD measurements alone, we obtain a constraint of $\xi > -0.033$ (i.e., an order of magnitude better than Planck-2018 + DESI), which further improves to $\xi > -0.0133$ when combined with DESI, SN, and CC data (both at the 95% CL). This latter combination restricts the ability of this class of models to fully resolve the H_0 tension, yielding $H_0 = 68.8 \pm 1.3$ km/s/Mpc, and suggests difficulties with structure growth constraints. Although this conclusion is subject to several caveats [56], the analysis of RSD data highlights the need for improved theoretical modeling to address RSD measurements effectively. For a more detailed analysis of the implications of structure formation growth in different IDE regimes (especially concerning the relation between the H_0 and S_8 tensions), we refer to the companion analysis presented in Ref. [57]. Therefore, we conclude by stressing that while the IDE model under consideration can resolve the Hubble tension based on background data, it faces challenges with large-scale structure probes sensitive to the dynamics of perturbations and the growth of cosmic structure, highlighting the need for theoretical and phenomenological improvements in this direction.

Acknowledgments—The authors express their gratitude to the referee for their valuable comments and suggestions, which have greatly enhanced the overall quality of the work. W. G. is supported by the Lancaster-Sheffield Consortium for Fundamental Physics under STFC Grant ST/X000621/1. M. A. S. received support from the CAPES scholarship. R. C. N. thanks the financial support from the Conselho Nacional de Desenvolvimento Científico e Tecnologico (CNPq, National Council for Scientific and Technological Development) under the Project No. 304306/2022-3, and the Fundação de Amparo à pesquisa do Estado do RS (FAPERGS, Research Support Foundation of the State of RS) for partial financial support under the Project No. 23/2551-0000848-3. E. D. V. is supported by a Royal Society Dorothy Hodgkin Research Fellowship. This article is based upon work from COST Action CA21136 Addressing observational tensions in cosmology with systematics and fundamental physics (CosmoVerse) supported by COST (European Cooperation in Science and Technology). We acknowledge IT Services at the University of Sheffield for the provision of services for high performance Computing.

[1] A. G. Riess *et al.*, Astrophys. J. Lett. **934**, L7 (2022).
[2] Y. S. Murakami, A. G. Riess, B. E. Stahl, W. D. Kenworthy, D.-M. A. Pluck, A. Macoretta, D. Brout, D. O. Jones, D. M. Scolnic, and A. V. Filippenko, J. Cosmol. Astropart. Phys. 11 (2023) 046.
[3] L. Breuval, A. G. Riess, S. Casertano, W. Yuan, L. M. Macri, M. Romaniello, Y. S. Murakami, D. Scolnic, G. S. Anand, and I. Soszyński, arXiv:2404.08038.
[4] N. Aghanim *et al.* (Planck Collaboration), Astron. Astrophys. **641**, A6 (2020); **652**, C4(E) (2021).
[5] This possibility appears increasingly unlikely given the extensive review of several potential sources of systematic error performed by the SH0ES Collaboration [1,6,7].
[6] A. G. Riess, G. S. Anand, W. Yuan, S. Casertano, A. Dolphin, L. M. Macri, L. Breuval, D. Scolnic, M. Perrin, and I. R. Anderson, Astrophys. J. Lett. **962**, L17 (2024).
[7] D. Brout and A. Riess, arXiv:2311.08253.
[8] E. Di Valentino, O. Mena, S. Pan, L. Visinelli, W. Yang, A. Melchiorri, D. F. Mota, A. G. Riess, and J. Silk, Classical Quantum Gravity **38**, 153001 (2021).
[9] E. Abdalla *et al.*, J. High Energy Astrophys. **34**, 49 (2022).
[10] A. R. Khalife, M. B. Zanjani, S. Galli, S. Günther, J. Lesgourgues, and K. Benabed, arXiv:2312.09814.
[11] N. Schöneberg, G. Franco Abellán, A. Pérez Sánchez, S. J. Witte, V. Poulin, and J. Lesgourgues, Phys. Rep. **984**, 1 (2022).
[12] L. Knox and M. Millea, Phys. Rev. D **101**, 043533 (2020).
[13] S. Vagnozzi, Universe **9**, 393 (2023).
[14] G. Efstathiou, Mon. Not. R. Astron. Soc. **505**, 3866 (2021).
[15] C. Krishnan, R. Mohayaee, E. O. Colgáin, M. M. Sheikh-Jabbari, and L. Yin, Classical Quantum Gravity **38**, 184001 (2021).
[16] R. E. Keeley and A. Shafieloo, Phys. Rev. Lett. **131**, 111002 (2023).
[17] S. Gariazzo, W. Giarè, O. Mena, and E. Di Valentino, arXiv:2404.11182.
[18] A. G. Adame *et al.* (DESI Collaboration), arXiv:2404.03000.
[19] A. G. Adame *et al.* (DESI Collaboration), arXiv:2404.03001.
[20] DESI Collaboration, arXiv:2404.03002.
[21] D. Wang, arXiv:2404.06796.
[22] M. Cortês and A. R. Liddle, arXiv:2404.08056.
[23] E. O. Colgáin, M. G. Dainotti, S. Capozziello, S. Pourojaghi, M. M. Sheikh-Jabbari, and D. Stojkovic, arXiv:2404.08633.
[24] W. Yin, arXiv:2404.06444.
[25] A. Pourtsidou and T. Tram, Phys. Rev. D **94**, 043518 (2016).
[26] E. Di Valentino, A. Melchiorri, and O. Mena, Phys. Rev. D **96**, 043503 (2017).
[27] S. Kumar and R. C. Nunes, Phys. Rev. D **96**, 103511 (2017).
[28] R. von Marttens, L. Lombriser, M. Kunz, V. Marra, L. Casarini, and J. Alcaniz, Phys. Dark Universe **28**, 100490 (2020).
[29] M. Lucca and D. C. Hooper, Phys. Rev. D **102**, 123502 (2020).
[30] Y. Zhai, W. Giarè, C. van de Bruck, E. Di Valentino, O. Mena, and R. C. Nunes, J. Cosmol. Astropart. Phys. 07 (2023) 032.
[31] A. Bernui, E. Di Valentino, W. Giarè, S. Kumar, and R. C. Nunes, Phys. Rev. D **107**, 103531 (2023).
[32] G. A. Hoerning, R. G. Landim, L. O. Ponte, R. P. Rolim, F. B. Abdalla, and E. Abdalla, arXiv:2308.05807.
[33] W. Giarè, Y. Zhai, S. Pan, E. Di Valentino, R. C. Nunes, and C. van de Bruck, arXiv:2404.02110.
[34] R. C. Nunes, S. Vagnozzi, S. Kumar, E. Di Valentino, and O. Mena, Phys. Rev. D **105**, 123506 (2022).
[35] W. Yang, S. Pan, O. Mena, and E. Di Valentino, J. High Energy Astrophys. **40**, 19 (2023).
[36] M. B. Gavela, L. Lopez Honorez, O. Mena, and S. Rigolin, J. Cosmol. Astropart. Phys. 11 (2010) 044.
[37] E. Di Valentino, A. Melchiorri, O. Mena, and S. Vagnozzi, Phys. Rev. D **101**, 063502 (2020).
[38] E. Silva, U. Zúñiga-Bolaño, R. C. Nunes, and E. D. Valentino, arXiv:2403.19590.
[39] E. Di Valentino, A. Melchiorri, O. Mena, and S. Vagnozzi, Phys. Dark Universe **30**, 100666 (2020).
[40] We regularize early-time superhorizon instabilities in the dynamics of cosmological perturbations [36,41] by setting $w = -1 + \epsilon$ and taking $\epsilon \simeq 0.0001 \to 0$.
[41] J. Valiviita, E. Majerotto, and R. Maartens, J. Cosmol. Astropart. Phys. 07 (2008) 020.
[42] D. Blas, J. Lesgourgues, and T. Tram, J. Cosmol. Astropart. Phys. 07 (2011) 034.
[43] J. Torrado and A. Lewis, J. Cosmol. Astropart. Phys. 05 (2021) 057.
[44] N. Aghanim *et al.* (Planck Collaboration), Astron. Astrophys. **641**, A5 (2020).
[45] N. Aghanim *et al.* (Planck Collaboration), Astron. Astrophys. **641**, A1 (2020).
[46] D. Brout *et al.*, Astrophys. J. **938**, 110 (2022).
[47] R. Jimenez and A. Loeb, Astrophys. J. **573**, 37 (2002).
[48] M. Moresco, L. Verde, L. Pozzetti, R. Jimenez, and A. Cimatti, J. Cosmol. Astropart. Phys. 07 (2012) 053.
[49] M. Moresco, Mon. Not. R. Astron. Soc. **450**, L16 (2015).
[50] M. Moresco, L. Pozzetti, A. Cimatti, R. Jimenez, C. Maraston, L. Verde, D. Thomas, A. Citro, R. Tojeiro, and D. Wilkinson, J. Cosmol. Astropart. Phys. 05 (2016) 014.
[51] To do so, we employ the MCEvidence package, which is publicly available [52,53] and can be accessed at the following link: https://github.com/yabebalFantaye/MCEvidence.
[52] A. Heavens, Y. Fantaye, E. Sellentin, H. Eggers, Z. Hosenie, S. Kroon, and A. Mootoovaloo, Phys. Rev. Lett. **119**, 101301 (2017).
[53] A. Heavens, Y. Fantaye, A. Mootoovaloo, H. Eggers, Z. Hosenie, S. Kroon, and E. Sellentin, arXiv:1704.03472.
[54] We note that this essentially means the model can fit both the large-scale structure data and SH0ES measurements simultaneously, without resulting in a poor fit. If one attempted the same with the ΛCDM model, it would also reduce the Hubble tension, but at the cost of significantly increasing the χ^2 (by ∼25) due to the discrepancy between the cosmological H_0 inference and the SH0ES measurement.
[55] B. Sagredo, S. Nesseris, and D. Sapone, Phys. Rev. D **98**, 083543 (2018).
[56] While robust, some caveats surrounding our analysis of RSD include the reliance on extrapolating linear models into regimes where they may not be valid, the absence of a quasilinear power spectrum in the IDE model that could potentially weaken the constraints on ξ, and the fact that, while distance measurements come from DESI, the RSD

measurements are sourced from various studies in the literature, each employing different approximations and methods.
[57] M. A. Sabogal, E. Silva, R. C. Nunes, S. Kumar, E. Di Valentino, and W. Giarè, arXiv:2408.12403.
[58] S. Alam *et al.*, Phys. Rev. D **103**, 083533 (2021).
[59] In the spirit of discussing all possibilities and cross-referencing our findings with different datasets, we refer readers to [31], where we tested the same model against some 2D BAO measurements extracted from the SDSS catalog. This dataset has recently gained research attention within the cosmology community. In this case, we observe a preference for a nonzero ξ that aligns well with the results obtained from DESI.

End Matter

Appendix: Comparing DESI and SDSS constraints—We present a quantitative comparison between results obtained using DESI and SDSS BAO measurements for the interacting dark energy model studied in this work. In particular, we consider two distinct datasets: (i) Planck-2018 + DESI—Planck temperature polarization and lensing likelihoods [4,44,45] in combination with the *DESI* BAO measurements obtained from observations of galaxies and quasars [18], and Lyman-α [19] tracers summarized in Table I of Ref. [20] (this dataset is labeled as "Planck-2018 + DESI" throughout the Letter). (ii) Planck-2018 + SDSS—Planck temperature polarization and lensing likelihoods [4,44,45] in combination with the SDSS BAO measurements from the final SDSS Collaboration compilation encompassing the eight distinct redshift intervals summarized in Table 3 of [58].

We note that both datasets focus on the same distance and expansion rate measurements, namely the isotropic BAO measurements of $D_V(z)/r_\mathrm{d}$ (where $D_V(z)$ and r_d denote the spherically averaged volume distance and sound horizon at baryon drag, respectively), as well as anisotropic BAO measurements of $D_M(z)/r_\mathrm{d}$ and $D_H(z)/r_\mathrm{d}$ [with $D_M(z)$ representing the comoving angular diameter distance and $D_H(z) = [c/H(z)]$ denoting the Hubble distance]. Both datasets have similar constraining power; therefore, combining them can be interesting to determine whether there is a consistent preference away from the ΛCDM model toward higher H_0. Additionally, it will help assess to what extent this preference is driven by new DESI BAO measurements.

Table III summarizes the observational constraints for the main baseline of the model, while Fig. 4 shows the marginalized probability contours in the H_0-ξ plane for both Planck-2018 + DESI and Planck-2018 + SDSS. From the joint analysis of Planck-2018 + SDSS, we find the lower limit $\xi > -0.389$ at 95% CL, indicating no concrete preference for an interaction in the dark sector. On the brighter side, we still observe a shift toward larger values of $H_0 \sim 69$ km/s/Mpc, which is in better agreement with SH0ES than a minimal ΛCDM model. In contrast, as discussed in the main text, the analysis of Planck-2018 + DESI data yields a substantial shift toward a nonvanishing energy-momentum flow from the DM to the DE sector $\xi = -0.32^{+0.30}_{-0.29}$ at 95% CL that further moves the value of H_0 toward local distance ladder estimates. Therefore, taking these results at face value, it appears that a significant part of the preference for nonzero ξ comes from DESI BAO data, while no preference for $\xi \neq 0$ is not found in SDSS data. However, we would like to emphasize that within the IDE framework of this work, there is no actual tension in the constraints obtained for Planck-2018 + SDSS and Planck-2018 + DESI. The SH0ES, Planck-2018 + DESI, and Planck-2018 + SDSS contours all overlap well within the 95% confidence level in the H_0-ξ plane; see also Fig. 4 [59].

TABLE III. Constraints at 68% (95%) CL on the parameters of the IDE model.

Parameter	Planck-2018 + DESI	Planck-2018 + SDSS
$10^2 \times \Omega_\mathrm{b}h^2$	2.243 ± 0.014	2.236 ± 0.013
$\Omega_\mathrm{c}h^2$	$0.079^{+0.025}_{-0.016}$	$0.101^{+0.016}_{-0.012}$
H_0	$70.8^{+1.4}_{-1.7}$	$68.92^{+0.96}_{-1.2}$
τ_reio	0.0555 ± 0.0074	0.0544 ± 0.0079
$\log(10^{10}A_\mathrm{s})$	3.045 ± 0.014	3.045 ± 0.016
n_s	0.9672 ± 0.0037	0.9650 ± 0.0037
ξ	$-0.32^{+0.18}_{-0.14}(-0.32^{+0.30}_{-0.29})$	$> -0.207(> -0.389)$

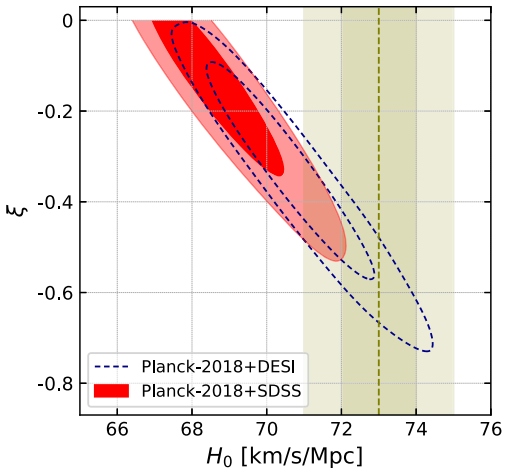

FIG. 4. 2D contours at 68% and 95% CL for the coupling parameter ξ and the Hubble parameter H_0, as inferred by the different combinations of Planck-2018, DESI, and SDSS data listed in the legend. The olive-green band represents the value of H_0 measured by the SH0ES Collaboration.